Molecular Biology of the Cell
Vol. 18, 1359–1365, April 2007

Conserved Actin Cysteine Residues Are Oxidative Stress Sensors That Can Regulate Cell Death in Yeast

Michelle E. Farah and David C. Amberg

Department of Biochemistry and Molecular Biology, State University of New York Upstate Medical University, Syracuse, NY 13210

Submitted August 16, 2006; Revised January 8, 2007; Accepted January 31, 2007
Monitoring Editor: Charles Boone

Actin's functional complexity makes it a likely target of oxidative stress but also places it in a prime position to coordinate the response to oxidative stress. We have previously shown that the NADPH oxidoreductase Oye2p protects the actin cytoskeleton from oxidative stress. Here we demonstrate that the physiological consequence of actin oxidation is to accelerate cell death in yeast. Loss of Oye2p leads to reactive oxygen species accumulation, activation of the oxidative stress response, nuclear fragmentation and DNA degradation, and premature chronological aging of yeast cells. The *oye2*Δ phenotype can be completely suppressed by removing the potential for formation of the actin C285-C374 disulfide bond, the likely substrate of the Oye2p enzyme or by treating the cells with the clinically important reductant *N*-acetylcysteine. Because these two cysteines are coconserved in all actin isoforms, we theorize that we have uncovered a universal mechanism whereby actin helps to coordinate the cellular response to oxidative stress by both sensing and responding to oxidative load.

INTRODUCTION

The accumulation of oxygen-containing free radicals in the cell results in oxidative stress conditions that can cause apoptosis and cellular aging. The actin cytoskeleton is an early target of cellular oxidative stress (Dalle-Donne *et al.,* 2001) and in certain disease conditions, the oxidative state of actin in the cell is very different from normal. For example, in sickle cell crisis, a major factor that contributes to the inflexibility of irreversibly sickled cells (ISCs) is the formation of an intracellular disulfide bond between C284 and C373 of β-actin (Shartava *et al.,* 1995; Bencsath *et al.,* 1996). We have previously shown that the yeast actin cytoskeleton is subject to the same form of oxidative damage as ISC actin. Our finding that an oxidoreductase called Oye2p (old yellow enzyme) regulates oxidation between C285 and C374 in *Saccharomyces cerevisiae* suggests that actin oxidation takes place in all eukaryotic cells and that the actin cytoskeleton is subject to redox regulation (Haarer and Amberg, 2004). That $act1^{C285A}$- and $act1^{C374A}$-bearing mutants are more resistant to oxidative stress than wild-type strains and that these alleles completely suppress the oxidative sensitivity of an old yellow enzyme (OYE) null strain proves that actin is a critical target for determining sensitivity to oxidative stress.

Actin's involvement in programmed cell death is gaining greater recognition in the apoptosis and cancer research fields (Rao and Li, 2004). Altering actin dynamics in lymphocytes by either stabilizing or destabilizing F-actin structures modulates apoptotic signaling upon withdrawal of growth factors (Posey and Bierer, 1999). In addition, during TNF-α apoptotic signaling, viral disruption at the β-actin locus dramatically reduces mitochondrial clustering and production of reactive oxygen species (ROS), indicating that actin participates in a programmed cell death program (Li *et al.,* 2004). Furthermore, hyperstabilization of actin by addition of a drug called jasplakinolide (Jas) induced apoptosis in HL-60 cells, and blocking actin polymerization inhibited camptothesin-induced apoptosis, suggesting that the polymerization status of the actin cytoskeleton is crucial to apoptotic initiation and progression (Rao *et al.,* 1999).

In recent years, the yeast model has been emerging as an important system to better understand the ancestrally conserved mechanisms of regulated cell death such as apoptosis, autophagy, and necrosis. The validity of the yeast model for studying programmed cell death is bolstered by the observations that yeast cells exhibit apoptotic markers in common with mammalian cells such as chromatin condensation, DNA fragmentation, phosphatidylserine exposure, and ROS accumulation (Madeo *et al.,* 1999). In *S. cerevisiae*, decreased actin dynamics has been shown to increase the accumulation of ROS (Gourlay *et al.,* 2004). Because the redox state of actin has been observed in some systems to be an important contributor to actin stability (Shartava *et al.,* 1995, 1997; Haarer and Amberg, 2004), in the current study we asked whether the oxidation state of actin's cysteines 285 and 374 was able to regulate cell death in *S. cerevisiae*. Our data suggest that the oxidoreductase Oye2p plays a prosurvival role in the cell by protecting the actin cytoskeleton from oxidation-induced hyperstabilization. Our data support a model in which the actin cytoskeleton is a central signaling component that couples the accumulation of ROS to programmed cell death.

This article was published online ahead of print in *MBC in Press* (http://www.molbiolcell.org/cgi/doi/10.1091/mbc.E06–08–0718) on February 7, 2007.

Address correspondence to: David Charles Amberg (ambergd@upstate.edu).

Abbreviations used: NAC, *N*-acetyl-L-cysteine; OYE, old yellow enzyme; ROS, reactive oxygen species.

MATERIALS AND METHODS

Construction of Strains and Media Conditions

All yeast strains used in this study are of the S288C background. Yeast strains are listed in Table 1. Standard methods were used for growth, sporulation, transformation, and genetic analysis of yeast (Amberg *et al.,* 2005).

Table 1. *Saccharomyces cerevisiae* strains used in this study

Name	Genotype	Source
DAY111x112	*MAT***a**/*MATα ura3-52/ura3-52 leu2Δ1/leu2Δ1 trp1Δ63/trp1Δ63 his3Δ200/his3Δ200*	D. Amberg
DAY127x128	*MAT***a**/*MATα ura3-52/ura3-52 leu2Δ1/leu2Δ1 trp1Δ63/trp1Δ63 his3Δ200/his3Δ200 oye2-Δ2::*HIS3*/oye2-Δ2::*HIS3 *oye3-Δ2::*TRP1*/oye3-Δ2::*TRP1	Haarer and Amberg (2004)
DAY111	*MAT***a** *ura3-52 leu2Δ1 trp1Δ63 his3Δ200*	Haarer and Amberg (2004)
DAY119	*MAT***a** *ura3-52 leu2Δ1 trp1Δ63 his3Δ200 oye2-Δ2::*HIS3	Haarer and Amberg (2004)
DAY123	*MAT***a** *ura3-52 leu2Δ1 trp1Δ63 his3Δ200 oye3-Δ2::*TRP1	Haarer and Amberg (2004)
DAY128	*MAT***a** *ura3-52 leu2Δ1 trp1Δ63 his3Δ200 oye2-Δ2::*HIS3 *oye3-Δ2::*TRP1	Haarer and Amberg (2004)
MDY11	*MAT***a** *ura3-52 leu2Δ1 trp1Δ63 his3Δ200 oye2-Δ2::*HIS3 *act1^{C374A}::HIS3*	This study
MDY13	*MAT***a** *ura3-52 leu2Δ1trp1Δ63 his3Δ200 oye2-Δ2::*HIS3 *act1^{C285A}::HIS3*	This study
DAY173	*MAT***a** *ura3-52 leu2Δ1 trp1Δ63 his3Δ200 oye2-Δ2::*HIS3 *oye3-Δ2::*TRP1 *act1^{C285A}::HIS3*	Haarer and Amberg (2004)
DAY175	*MAT***a** *ura3-52 leu2Δ1 trp1Δ63 his3Δ200 oye2-Δ2::*HIS3 *oye3-Δ2::*TRP1 *act1^{C374A}::HIS3*	Haarer and Amberg (2004)
DAY169	*MAT***a** *ura3-52 leu2Δ1 trp1Δ63 his3Δ200 act1^{C374A}::HIS3*	Haarer and Amberg (2004)
DAY171	*MAT***a** *ura3-52 leu2Δ1 trp1Δ63 his3Δ200 act1^{C285A}::HIS3*	Haarer and Amberg (2004)
BHY313	*MATα his3Δ1 lys2Δ0 uraΔ0 act1-123::klURA3 mfa1Δ::P$_{MFA1}$-sphis5+, can1Δ*	B. Haarer

Generation of rho^0 Mutants

The method used to generate *rho^0* strains is as described (Goldring *et al.*, 1970). In addition to streaking all colonies to YP + 3% glycerol to confirm lack of mitochondrial respiratory function, DAPI staining was performed as described to confirm the complete absence of mitochondrial DNA (Amberg *et al.*, 2005).

Detection of Accumulation of ROS

Cultures were grown to logarithmic phase (about 3×10^7 cells/ml) and ROS were detected in vivo with the ROS-sensing dye dichlorodihydrofluorescein diacetate (H_2DCFDA; Sigma, St. Louis, MO) as previously described (Madeo *et al.*, 1999), except the cells were incubated for 3.5 h. Cells that appeared fluorescent in the FITC channel were scored as ROS positive. Cells (n = 500) were quantified for each experiment. The experiment was repeated at least three independent times for all strains, the number of cells that appeared fluorescent was averaged, and SDs were calculated.

Microscopy

The staining of the actin cytoskeleton and microscopy methods were performed as described (Amberg *et al.*, 2005).

Localization of GFP-Yap1p

The *URA3*-marked, low copy CEN vector pGFP-Yap1p was obtained from the Moie-Rowley lab (Coleman *et al.*, 1999). Transformed cells were grown in 3 ml SC-Ura medium until cells reach a density of $\sim 1 \times 10^8$ cells/ml. Cells were stained with 0.5 μg/ml DAPI for 15 min and observed for green fluorescent protein (GFP) fluorescence on a Zeiss Axioskop 2 MOT microscope (Thornwood, NY; Amberg *et al.*, 2005). Two hundred cells of each strain were scored for nuclear GFP-Yap1p localization.

Detection of Chromatin Fragmentation

DAPI staining was used to detect changes in nuclear morphology. Cells were grown in YPD medium to logarithmic phase (at a density of 3×10^7 cells/ml) and stained as described (Amberg *et al.*, 2005). Two hundred cells were quantified for the appearance of fragmented nuclei, and the experiment was repeated three independent times.

Detection of DNA Fragmentation

Cells were grown in YPD medium to logarithmic phase (3×10^7 cells/ml) and then fixed on a slide according to an immunofluorescence protocol (Amberg *et al.*, 2005). Cells were then permeabilized with a solution of 0.1% Triton X-100 and 0.1% sodium citrate. After this, the In Situ Cell Death Detection Kit, Fluorescein (Susin *et al.*, 1999) was used to label nicked DNA ends. Cells were then mounted in immunofluorescence mounting solution containing DAPI (Amberg *et al.*, 2005) and visualized by fluorescence microscopy.

Actin Staining of N*-acetyl-*L*-Cysteine–treated Cells*

While cells were growing in YPD in log phase, *N*-acetyl-L-cysteine (NAC) was added to a final concentration of 31 mM, and the cells were incubated for an additional 5.5 h. Cells were fixed and stained with rhodamine phalloidin as described (Amberg *et al.*, 2005).

Determination of Cell Viability

A fresh colony of each strain was inoculated into 5 ml of YPD in a well-aerated culture tube. For the length of the experiment, cultures were maintained on a rotating drum in a 30°C incubator. At the indicated time points, cells were gently sonicated with a Branson sonifier 450 (Branson Ultrasonics, Danbury, CT), and duplicate serial dilutions were made in YPD. The cells were diluted by a total factor of 10^6 of which 100 μl was plated onto YPD medium. Cell densities were obtained by making two 1:100 dilutions from each culture and then counting the cell numbers in duplicate in a hemacytometer. When a maximum cell density was obtained, this number was used as the cell density for all subsequent calculations of cell viability.

Cell viability was calculated as follows: Average colony forming units/maximum average cell density = % viability at each time point.
Each experiment was repeated three times.

For the viability experiments that utilized NAC, 5-ml cultures of cells were grown to stationary phase and at day 2, and the cultures were split into separate tubes (control and experimental). Cells were plated at days 2, 5, 8, 11, 14, and 18. An aqueous solution of NAC was added to a final concentration of 31 mM to cultures at either day 4 or day 6. An equivalent volume of water was added to the control sample. The fraction of viable cells was calculated as described above.

Statistical Methods

The calculation of the arithmetic mean, $\bar{x}$, was done as follows:

$$\bar{x} = \frac{1}{N}\sum_{i=1}^{N} x_i = \frac{x_1 + x_2 + \cdots + x_N}{N}$$

where x_N represents each individual value and n is the total number of values.

The calculation of the SD, σ, was performed as follows:

$$\sigma = \sqrt{\frac{1}{N}\sum_{i=1}^{N} (x_i - \bar{x})^2}$$

where σ is the SD, N is the total number of values, $\bar{x}$ is the arithmetic mean, and x_i is each individual value.

RESULTS

The Accumulation of ROS in Cells Lacking Oye2p Is Suppressed by act1^{C285A} and act1^{C374A}

ROS are central mediators of apoptosis in yeast and mammalian cells (Madeo *et al.*, 1999; Chandra *et al.*, 2000), being both necessary and sufficient to drive cells into programmed cell death (Madeo *et al.*, 1999). We have previously shown that *oye2*Δ cells are sensitive to external sources of oxidative stress and that the recovery of their actin cytoskeleton and growth after oxidative stress is delayed in comparison to wild-type cells. Here we asked whether *oye2*Δ cells have elevated levels of ROS in vivo by quantifying the percent-

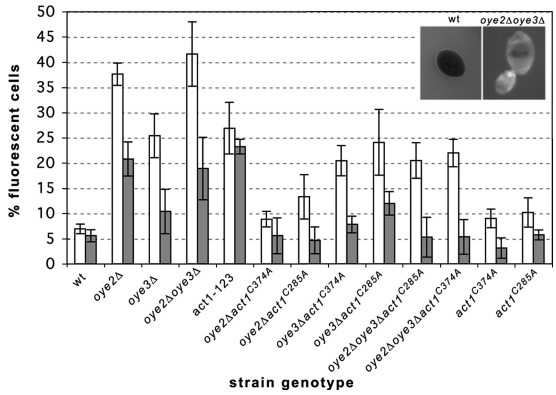

Figure 1. Actin oxidation in *oye*Δ cells leads to ROS accumulation. Logarithmically growing cells were stained for 3.5 h with the ROS-sensing dye H_2DCFDA, and the percentages of fluorescent cells was determined. □, *rho*$^+$ cells; ▨, *rho*^{0} cells. The averages and SDs reported are for three to four experiments. Left inset, example of an ROS-negative wild-type cell; right inset, example of an ROS-positive *oye*Δ cell.

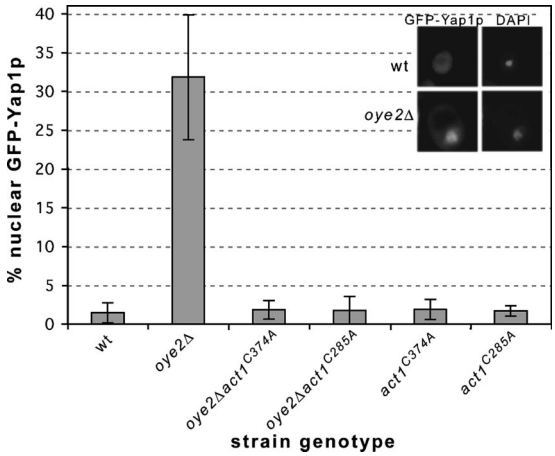

Figure 2. In the absence of Oye2p, actin oxidation activates the oxidative stress response. The oxidative stress responsive transcription factor Yap1p was expressed as a GFP fusion in various mutants and the percentages of cells with nuclear GFP-Yap1p was quantified by fluorescence microscopy. Nuclei were identified by DAPI staining. The results reported are for three experiments (n = 500 per experiment). Top insets, wild-type cell; bottom insets, oxidatively stressed *oye2*Δ cell.

ages of logarithmically growing cells that stain with the fluorescent, ROS indicator dye, H_2DCFDA. Examples of ROS negative wild-type versus ROS-positive *oye2*Δ cells are shown in the inset of Figure 1. To confirm that the ROS-sensing dye, H_2DCFDA, was specifically reacting with ROS in our cells, we showed that addition of the antioxidant NAC to the *oye2*Δ cells blocked H_2DCFDA-induced fluorescence (our unpublished observations). As shown in Figure 1, there is an ~30 and 20% increase in the number of H_2DCFDA reactive cells in *oye2*Δ and *oye3*Δ cells, respectively, compared with wild-type cultures. In an *oye2*Δ strain, but not the *oye3*Δ strain, we were able to suppress increased ROS levels with either the *act1*^{C285A} or the *act1*^{C374A} alleles. These data suggest that Oye2p, but not Oye3p, is playing a specific role in protecting cells from an elevation of ROS that is in fact induced by the oxidation of the C285-C374 cysteine pair in actin. Consistent with these observations, our previous studies showed that Oye3p is unable to interact with actin and that *oye3*Δ cells have a normal actin cytoskeleton (Haarer and Amberg, 2004). The *oye3*Δ strain does show an elevation in ROS-positive cells that appears to be unrelated to actin oxidation. Consistent with these observations, the *oye2*Δ *oye3*Δ *act1*^{C374A} and *oye2*Δ *oye3*Δ *act1*^{C285A} strains have ROS levels equivalent to that of the *oye3*Δ strain. To examine the potential role of a direct interaction between actin and Oye2p, in regulating the in vivo accumulation of ROS, we examined a strain expressing a mutant form of actin (act1-123p) that we previously showed has a reduced affinity for Oye2p (Haarer and Amberg, 2004). As expected, the *act1-123* strain showed a comparable percentage (27%) of ROS-positive cells to the *oye2*Δ strain.

Mitochondria have been accepted as the major source of ROS generation in the cell, specifically stemming from the electron transfer complexes of the respiratory chain (Fleury *et al.*, 2002). To examine whether the mitochondrial respiratory chain is the source of oxygen-containing free radicals in our ROS-elevated mutants, we generated strains lacking mitochondrial DNA (*rho*^{0}). These strains were tested for lack of growth on glycerol (a nonfermentable carbon source) and confirmed by DAPI staining to be devoid of mitochondrial DNA (data not shown) and are therefore lacking a functional mitchondrial respiratory chain. The loss of mitochondrial function was especially useful in identifying the major source of ROS generated in cells bearing the F-actin–stabilizing *act1–159* allele (Gourlay *et al.*, 2004). As shown in Figure 1, ROS-accumulating cells in *oye2*Δ and *oye3*Δ cultures were decreased by approximately half, indicating that half of the ROS in OYE-lacking mutants are generated from an origin other than the electron transport chain. We stained the actin cytoskeleton of *rho*^{0} *oye2*Δ*oye3*Δ cells in order to examine if this level of oxidative stress was sufficient to cause oxidation-mediated stabilization of the actin cytoskeleton. We found that there was a partial suppression of the hyperstabilized actin phenotype of the OYE-lacking mutants (our unpublished observations) consistent with the observed decrease in ROS levels. As with our *rho*$^+$ mutants, the number of *rho*^{0} *oye2*Δ cells with elevated ROS was suppressed to wild-type levels by both *act1*^{C285A} and *act1*^{C374A}. This suggests that the oxidative status of these cysteine residues of actin, and the consequent stabilization of the actin network, are key events in the mechanism governing ROS generation from both mitochondrial and nonmitochondrial sources.

Yap1p is a transcription factor that translocates to the nucleus upon exposure to oxidative stress (Coleman *et al.*, 1999). It contains a carboxy-terminal cysteine-rich domain (c-CRD) that senses cytoplasmic oxidative stress and is necessary for cellular viability upon addition of external oxidants (Kuge *et al.*, 1997; Wemmie *et al.*, 1997). Furthermore, age-induced cell death has been shown to be delayed in Yap1p-overexpressing strains (Herker *et al.*, 2004). As a second important indicator of oxidative stress, we found that in ~32% of *oye2*Δ cells, GFP-Yap1p is localized to the nucleus in early stationary phase cells, whereas this nuclear localization pattern was observed in <1% of a comparable culture of wild-type cells (Figure 2). Importantly, in our double mutants *oye2*Δ *act1*^{C285A} and *oye2*Δ *act1*^{C374A} nuclear accumulation of Yap1p is suppressed to wild-type levels. These results indicate that in the absence of Oye2p, normal cellular levels of ROS lead to actin oxidation and a perception that the cell is under oxidative stress. This actin oxidation appears to trigger an elevation of ROS and in this way, actin appears to be both a sensor and an effector of ROS elevation.

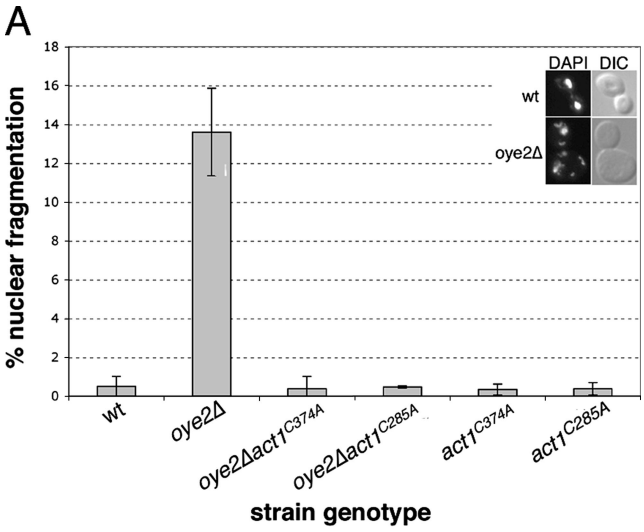

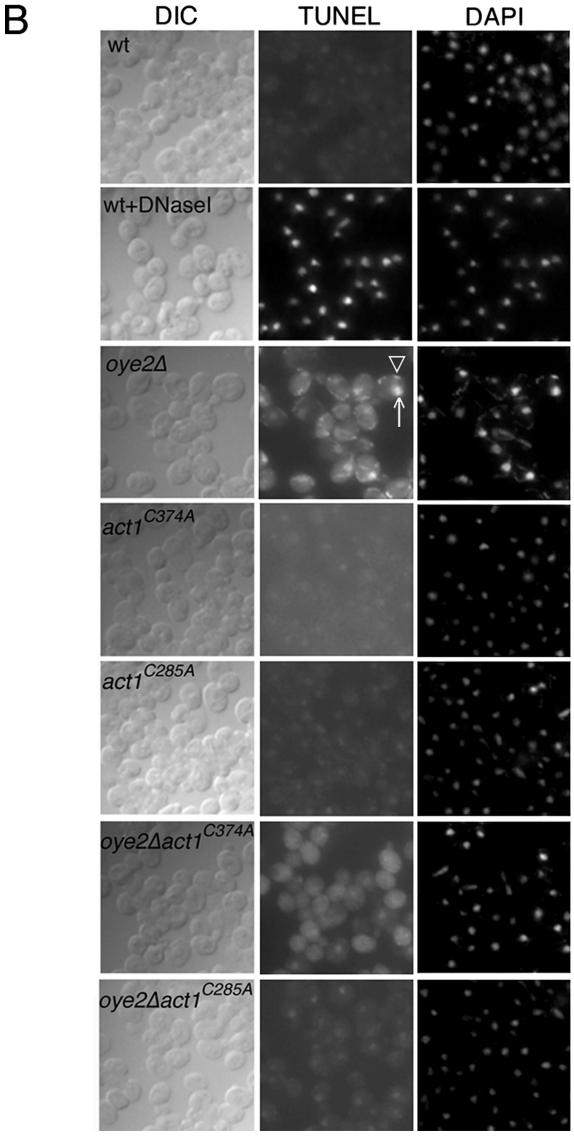

Figure 3. In the absence of Oye2p, cells show nuclear fragmentation and DNA degradation. (A) DAPI staining was performed on logarithmically growing cells, and the percentages of cells displaying nuclear fragmentation for each strain is shown. The results reported are for three independent experiments (n = 200 per experiment). Examples of cells displaying normal nuclear morphology (wild type) versus fragmented nuclei (*oye2*Δ) are shown in the inset on the top right. (B) TUNEL staining was performed on logarithmically growing cells. Each panel displays a random field of cells from cultures of the indicated genotypes. Left, DIC staining; middle, TUNEL staining; right, DAPI staining. As a positive control, wild-type cells were treated with 3 U/ml Dnase I for 20 min at room temperature (wt+DNaseI). White arrow, nuclear staining; white arrowhead, mitochondrial staining.

Nuclear and DNA Fragmentation in OYE2*-lacking Cells Is Suppressed by the act1^{C285A} and act1^{C374A} Alleles*

To assess whether ROS accumulation in *oye2*Δ cells is associated with apoptotic markers, we tested for an increase in nuclear/chromatin fragmentation and DNA degradation. DAPI staining revealed that *oye2*Δ cells had an increase in the percentage of cells containing fragmented nuclei: ~14% of *oye2*Δ cells showed nuclear fragmentation compared with <1% of wild-type cells (see Figure 3A). As expected, the positive control (wild-type cells treated for 200 min with 3 mM H_2O_2) also showed increased chromatin fragmentation (Madeo *et al.*, 1999). As shown in Figure 3A, the fragmentation observed in *oye2*Δ cells was completely suppressed by the *act1^{C285A}* and *act1^{C374A}* alleles.

In addition to DAPI staining, a TUNEL assay that is used to detect free 3′-OH ends of DNA (Gavrieli *et al.*, 1992; Madeo *et al.*, 1997) was used to examine whether the cellular DNA in the *oye2*Δ mutant was intact. DNase-I treatment of wild-type cells showed that the TUNEL assay accurately identified cells that exhibited an increase in free DNA ends (Figure 3B). We further showed that *oye2*Δ cells, relative to wild-type cells, displayed a large increase in the intensity of nuclear TUNEL staining (as a punctate dot; see white arrow) as well as mitochondrial TUNEL staining (see white arrowhead for an example). In contrast, the TUNEL staining of the *oye2*Δ*act1^{C285A}* and *oye2*Δ*act1^{C374A}* double mutants was nearly identical to wild type, indicating that DNA fragmentation in *oye2*Δ cells was also suppressed by the *act1^{C285A}* and *act1^{C374A}* alleles.

Chronological Aging of OYE-lacking Mutants Is Suppressed by act1^{C285A} and act1^{C374A}

It has previously been observed that aging yeast cells display an apoptotic phenotype, showing markers such as increased ROS accumulation, DNA degradation, extracellular phosphatidylserine exposure, and yeast caspase activation (Herker *et al.*, 2004). To determine if the observed ROS elevation in *oye*-deficient cells is triggering cell death, we monitored the viability of our strains maintained in YPD over a period of 18 d. The survival of yeast strains varies dramatically in different media conditions. Wild-type cells that are grown in synthetic complete minimal medium lose viability after 10 d (our unpublished observations). In contrast, cells that are grown and maintained in stationary phase on rich media can maintain viability for weeks (Sinclair *et al.*, 1998; Chen *et al.*, 2005). We found that there was a rapid decline in the viability of our *oye2*Δ cells compared with wild-type cells (Figure 4). During 18 d at stationary phase, both the *oye2*Δ and *oye2*Δ *oye3*Δ cell viabilities dramatically decreased from day 2 to day 5, reaching <20% by day 18 compared with 70% viability observed for wild-type cells. Note that the loss of *OYE3* appears to have little additive effect, suggesting that the loss of *OYE2* alone is causing the observed lowering in cell viability. Importantly,

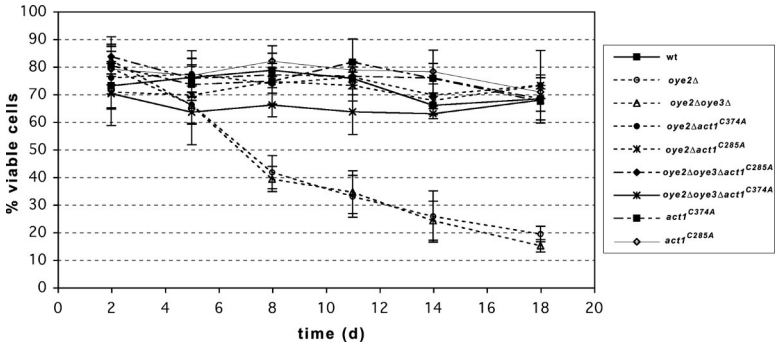

Figure 4. In the absence of Oye2p, actin oxidation leads to premature aging and cell death. Strains were grown to and maintained in stationary phase for 18 d. On the indicated days, cells were plated and the percentages of viable cells were determined based on colony-forming units per total cells. The averages and SDs were calculated from three experiments, where n = 400, n being the number of cell bodies plated.

the premature aging of the *oye2*Δ (and the *oye2*Δ*oye3*Δ cells) was suppressed by both the $act1^{C285A}$ and $act1^{C374A}$ alleles. These data support our model that in the absence of Oye2p, oxidation of actin's cysteine residues, and the resulting elevation of ROS, leads to premature aging and cell death.

The Antioxidant NAC Suppresses the Actin Defects and Loss of Viability Observed in oye-lacking Mutants

NAC is an antioxidant that is emerging as an important therapeutic agent for the treatment of many conditions. Importantly, NAC is in stage II clinical trials as a treatment for sickle cell patients. It is believed to act by reducing the oxidation of thiol groups in the β -actin and spectrin of irreversibly sickled RBCs restoring plasiticity to the cortical cytoskeleton (Goodman, 2004; Gibson *et al.*, 1998).

To ask if NAC could reverse the effects of actin oxidation in yeast, we examined the phenotype of *oye2*Δ*oye3*Δ cells after treatment with NAC. As can be seen in Figure 5A, the characteristic actin organization defects of the OYE deficient strain (hyperstabilization of actin cables and patches) were suppressed by the addition of NAC. We next tested whether the accelerated death of the *oye2*Δ cells in stationary phase could be suppressed by the addition of 31 mM NAC (Figure 5B). The addition of NAC at day 4 increased the percentage of *oye2*Δ viable cells at day 5 from 78 to 92%. By day 8, addition of NAC at either day 4 or day 6 increased untreated *oye2*Δ viability from 63% to 82 and 86%, respectively. However, after day 8, the viability of both NAC-treated *oye2*Δ and wild-type cultures rapidly drops off perhaps as a consequence of NAC or NAC byproduct toxicity. In support of this observation, another group has reported that at concentrations of NAC equal to or greater than 10 mM, the ability of the compound to promote growth in yeast mutants lacking superoxide dismutase was less than that observed at lower concentrations (Zyracka *et al.*, 2005). This indicates that at high concentrations, the antioxidant is toxic to yeast. However, in our viability experiments we have used a relatively high concentration of NAC because it most dramatically suppressed the hyperstable actin phenotype associated with the OYE-lacking mutant, whereas a lower concentration (6.2 mM) did not (our unpublished observations). Nonetheless, it appears that NAC can transiently protect the actin cytoskeleton of yeast from oxidative stress and from actin oxidation-induced cell death 8 d into stationary phase.

DISCUSSION

Actin is perhaps one of the most functionally diverse proteins in eukaryotic cells. Traditionally the actin cytoskeleton is thought of as playing structural and organizational roles as well as a being a direct participant in a wide range of motility processes. Recently actin has also been found to be involved in many nuclear processes as well including regulation of chromatin structure and transcription (Olave *et al.*, 2002; Bettinger *et al.*, 2004; Percipalle and Visa, 2006). This functional diversity makes the actin cytoskeleton an ideal candidate for integrating signaling between diverse cellular processes. Previous work has not extended actin's functions to include signaling but the results presented here show that a distinct change in the actin oxidation state activates an oxidative stress response that can culminate in programmed cell death during aging. Concerning the work presented here, it has become appreciated that the proper regulation of actin dynamics is an important determinant of cell survival; hyperstabilization of actin filaments leads to an apoptotic phenotype followed by programmed cell death in both yeast and mammalian cells (Rao *et al.*, 1999; Gourlay *et al.*, 2004)

We have furthered these findings by showing that cysteines 285 and 374 of actin are important physiological sensors of intracellular oxidative stress and are regulators of programmed cell death during chronological aging. Specifically, the $act1^{C285A}$ and $act1^{C374A}$ alleles are able to suppress the intracellular accumulation of ROS, Yap1p nuclear localization, nuclear fragmentation, DNA degradation, and accelerated cell death observed in *oye*Δ cells. We have also shown that both the hyperstabilized actin phenotype and rapid decline of chronologically aging *oye* cultures is suppressed by treatment with the clinically relevant antioxidant NAC. NAC is becoming recognized as an important treatment for HIV infection (Kalebic *et al.*, 1991; Roederer *et al.*, 1991; Herzenberg *et al.*, 1997), cancer (Morini *et al.*, 1999), neurodegenerative diseases (Deigner *et al.*, 2000), and other diseases and conditions. It is believed to function by protecting against cell death/as a promoter of cell survival (Mayer and Noble, 1994). Importantly, it is currently in phase II trials for the treatment for sickle cell crisis (Goodman, 2004). Its efficacy in treating sickle cell crisis is based on its ability to reduce C284-C373 oxidized actin and return proper plasticity to the red blood cell (RBC) cytoskeleton (Gibson *et al.*, 1998). The results reported here further suggest that NAC may act by suppressing an actin-induced cell death pathway. Erythrocytes are capable of undergoing a form of apoptosis known as eryptosis. In patients with sickle cell anemia, erythrocytes have been shown to have a 6 d half-life, compared with the 60 d half-life of normal RBCs (Benjamin and Manning, 1986). It is also worth noting that sickle cells generate twice the amount of ROS as control RBCs, an observation similar to that of *OYE*-lacking mutants (Hebbel *et al.*, 1982). Future studies of the mechanism of action of NAC in the treatment of sickle cell anemia and other diseases may find that the oxidative state of actin plays a large

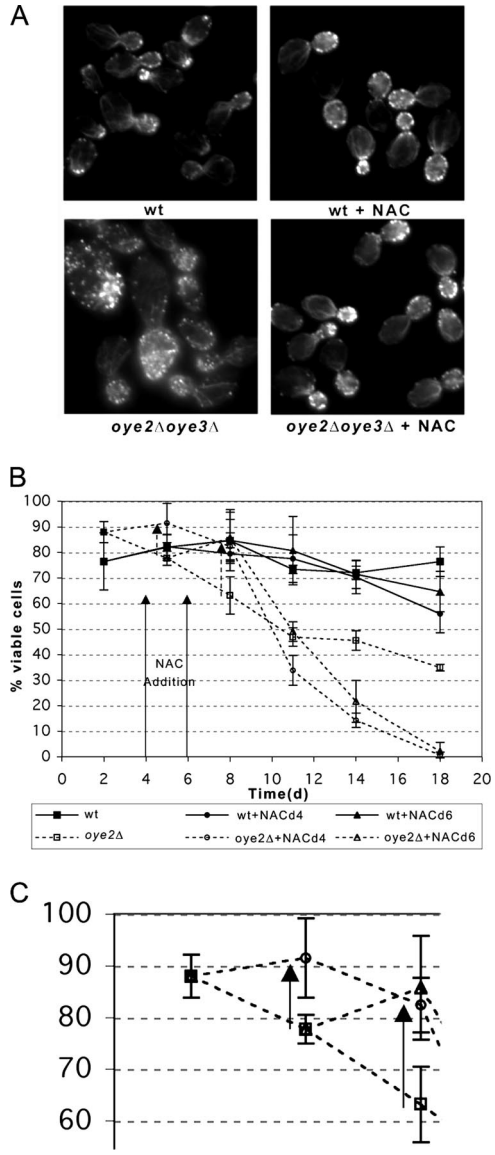

Figure 5. *N*-acetyl-L-cysteine (NAC) suppresses the actin organization and accelerated cell death phenotype of *oye2*Δ cells. (A) NAC was added to logarithmically growing cultures at a final concentration of 31 mM for 5.5 h, after which the cells were fixed, stained with rhodamine phalloidin and visualized by fluorescence microscopy. (B) NAC was added at a final concentration of 31 mM to stationary cultures on days 4 or 6 (indicated by arrows). Cells were removed at the indicated time points, dilutions were plated, and percent viability was calculated based on colony-forming units per total cell density. The arrows with dotted lines show the increases in viability at day 5 for NAC addition at day 4 and at day 8 for NAC addition at days 4 and 6. (C) The box highlights a portion of Figure 4B, with only the *oye2*Δ samples highlighted at days 2, 5, and 8.

part in the determination of survival of mammalian cells and that a key target of NAC is oxidized actin.

If actin's cysteines 285 and 374 can become disulfide-bonded and ultimately cause cell death, then why have they been coconserved in all eukaryote actin isoforms? We theorize that it may be to aid in the destruction of unfit cells that have accumulated excessive ROS and intracellular oxidative damage. In support of this theory of adaptive aging, superoxide has been proposed to mediate an altruistic aging and death program that leads to the death of >90% of a yeast population to allow for the survival of fitter/healthier cells (Fabrizio *et al.*, 2004).

To begin to understand the cellular mechanisms by which ROS are being generated in *oye2*Δ cells, we have used cells lacking a functional respiratory chain to show that mitochondrial ROS account for approximately half of the total ROS accumulation in *oye2*Δ cells. Many studies have shown that mitochondria and actin functionally interact. Regulation of actin dynamics is required for proper mitochondrial inheritance and for maintenance of mitochondrial morphology (Boldogh *et al.*, 2001; Okamoto and Shaw, 2005). The actin-depolymerizing protein gelsolin has been shown to inhibit the activity of the voltage-dependent anion channel (VDAC), the major channel in the outer membrane of mitochondria that regulates superoxide release, thereby preventing apoptotic mitochondrial changes in mammalian cells (Kusano *et al.*, 2000). Actin itself has been shown to regulate apoptotic changes in *Neurospora crassa*, where monomeric actin, not the filamentous form, appears to regulate this channel's activity (Xu *et al.*, 2001). Yeast also contains the VDAC in their mitochondria (Forte *et al.*, 1987). One can easily imagine that the release of ROS through pores in the mitochondrial membrane of yeast and mammalian cells may be an event that is regulated by the dynamic state of actin. In our model, actin would be further targeted by mitochondrial ROS, and this would lead to greater stabilization of actin and even more spilling of ROS from mitochondria in a positive feedback loop leading to cell death. However, half of the ROS generated in *oye*Δ cells appears to derive from nonmitochondrial sources. We do not currently know the source of this pool of ROS, but it is tempting to speculate that oxidized actin, interacting with cellular redox systems, directly results in the production of ROS.

Our findings that both nuclear and mitochondrial DNA in OYE2-lacking cells are stained with TUNEL suggests that the apoptotic mechanism involves the breakdown of both nuclear and mitochondrial DNA. Although the TUNEL assay is primarily used to label fragmented nuclear DNA, we have shown that fragmented mitochondrial DNA may also be labeled by this method. We speculate that the accumulation of ROS in the Oye2p-lacking mutant leads to mitochondrial fragmentation and that the converse may also be true. Indeed, it has been noted in mammalian cells that ROS generated from mitochondria are able to attack mitochondrial DNA, causing large-scale mtDNA deletions (Hayakawa *et al.*, 1992).

Although some of the molecular details remain to be elucidated, the work presented here is consistent with a model in which cellular oxidative load is measured via the oxidative formation of the C285-C374 disulfide bond of actin. Under normal levels of ROS, old yellow enzyme 2 is able to keep pace in reducing the disulfide but when the load becomes too high, or perhaps if Oye2p is inhibited or the NADPH levels required to keep Oye2p reduced become limiting, the resulting accumulation of oxidized actin results in stabilization of the actin cytoskeleton. This in turn triggers further elevation of ROS, in part via spilling from the mitochondria, leading to greater oxidation and stabilization of actin, thereby establishing a positive feedback loop that ultimately leads to cell death.

ACKNOWLEDGMENTS

We thank B. Haarer for helpful suggestions, P. Kane and Y. Huang for helpful discussions and ideas, and all members of the Amberg laboratory for helpful input, and to the Kane laboratory for use of reagents. Finally, we thank S. Moye-Rowley for the GFP-YAP1 vector and K. Ayscough and C. Gourlay for technical assistance. This research was supported by National Institutes of Health Grant GM-56189.

REFERENCES

Amberg, D. C., Burke, D. J., and Strathern, J. N. (2005). Methods in Yeast Genetics: A Cold Spring Harbor Laboratory Course Manual, Cold Spring Harbor, NY: Cold Spring Harbor Laboratory Press.

Bencsath, F. A., Shartava, A., Monteiro, C. A., and Goodman, S. R. (1996). Identification of the disulfide-linked peptide in irreversibly sickled cell beta-actin. Biochemistry *35*, 4403–4408.

Benjamin, L. J., and Manning, J. M. (1986). Enhanced survival of sickle erythrocytes upon treatment with glyceraldehyde. Blood *67*, 544–546.

Bettinger, B. T., Gilbert, D. M., and Amberg, D. C. (2004). Actin up in the nucleus. Nat. Rev. Mol. Cell Biol. *5*, 410–415.

Boldogh, I. R., Yang, H. C., and Pon, L. A. (2001). Mitochondrial inheritance in budding yeast. Traffic *2*, 368–374.

Chandra, J., Samali, A., and Orrenius, S. (2000). Triggering and modulation of apoptosis by oxidative stress. Free Radic. Biol. Med. *29*, 323–333.

Chen, Q., Ding, Q., and Keller, J. N. (2005). The stationary phase model of aging in yeast for the study of oxidative stress and age-related neurodegeneration. Biogerontology *6*, 1–13.

Coleman, S. T., Epping, E. A., Steggerda, S. M., and Moye-Rowley, W. S. (1999). Yap1p activates gene transcription in an oxidant-specific fashion. Mol. Cell. Biol. *19*, 8302–8313.

Dalle-Donne, I., Rossi, R., Milzani, A., Di Simplicio, P., and Colombo, R. (2001). The actin cytoskeleton response to oxidants: from small heat shock protein phosphorylation to changes in the redox state of actin itself. Free Radic. Biol. Med. *31*, 1624–1632.

Deigner, H. P., Haberkorn, U., and Kinscherf, R. (2000). Apoptosis modulators in the therapy of neurodegenerative diseases. Expert Opin. Investig. Drugs *9*, 747–764.

Fabrizio, P., Battistella, L., Vardavas, R., Gattazzo, C., Liou, L. L., Diaspro, A., Dossen, J. W., Gralla, E. B., and Longo, V. D. (2004). Superoxide is a mediator of an altruistic aging program in *Saccharomyces cerevisiae*. J. Cell Biol. *166*, 1055–1067.

Fleury, C., Mignotte, B., and Vayssiere, J. L. (2002). Mitochondrial reactive oxygen species in cell death signaling. Biochimie *84*, 131–141.

Forte, M., Adelsberger-Mangan, D., and Colombini, M. (1987). Purification and characterization of the voltage-dependent anion channel from the outer mitochondrial membrane of yeast. J. Membr. Biol. *99*, 65–72.

Gavrieli, Y., Sherman, Y., and Ben-Sasson, S. A. (1992). Identification of programmed cell death in situ via specific labeling of nuclear DNA fragmentation. J. Cell Biol. *119*, 493–501.

Gibson, X. A., Shartava, A., McIntyre, J., Monteiro, C. A., Zhang, Y., Shah, A., Campbell, N. F., and Goodman, S. R. (1998). The efficacy of reducing agents or antioxidants in blocking the formation of dense cells and irreversibly sickled cells in vitro. Blood *91*, 4373–4378.

Goldring, E. S., Grossman, L. I., Krupnick, D., Cryer, D. R., and Marmur, J. (1970). The petite mutation in yeast. Loss of mitochondrial deoxyribonucleic acid during induction of petites with ethidium bromide. J. Mol. Biol. *52*, 323–335.

Goodman, S. R. (2004). The irreversibly sickled cell: a perspective. Cell Mol. Biol. (Noisy-le-grand) *50*, 53–58.

Gourlay, C. W., Carpp, L. N., Timpson, P., Winder, S. J., and Ayscough, K. R. (2004). A role for the actin cytoskeleton in cell death and aging in yeast. J. Cell Biol. *164*, 803–809.

Haarer, B. K., and Amberg, D. C. (2004). Old yellow enzyme protects the actin cytoskeleton from oxidative stress. Mol. Biol. Cell *15*, 4522–4531.

Hayakawa, M., Hattori, K., Sugiyama, S., and Ozawa, T. (1992). Age-associated oxygen damage and mutations in mitochondrial DNA in human hearts. Biochem. Biophys. Res. Commun. *189*, 979–985.

Hebbel, R. P., Eaton, J. W., Steinberg, M. H., and White, J. G. (1982). Erythrocyte/endothelial interactions in the pathogenesis of sickle-cell disease: a "real logical" assessment. Blood Cells *8*, 163–173.

Herker, E., Jungwirth, H., Lehmann, K. A., Maldener, C., Frohlich, K. U., Wissing, S., Buttner, S., Fehr, M., Sigrist, S., and Madeo, F. (2004). Chronological aging leads to apoptosis in yeast. J. Cell Biol. *164*, 501–507.

Herzenberg, L. A., De Rosa, S. C., Dubs, J. G., Roederer, M., Anderson, M. T., Ela, S. W., and Deresinski, S. C. (1997). Glutathione deficiency is associated with impaired survival in HIV disease. Proc. Natl. Acad. Sci. USA *94*, 1967–1972.

Kalebic, T., Kinter, A., Poli, G., Anderson, M. E., Meister, A., and Fauci, A. S. (1991). Suppression of human immunodeficiency virus expression in chronically infected monocytic cells by glutathione, glutathione ester, and N-acetylcysteine. Proc. Natl. Acad. Sci. USA *88*, 986–990.

Kuge, S., Jones, N., and Nomoto, A. (1997). Regulation of yAP-1 nuclear localization in response to oxidative stress. EMBO J. *16*, 1710–1720.

Kusano, H., Shimizu, S., Koya, R. C., Fujita, H., Kamada, S., Kuzumaki, N., and Tsujimoto, Y. (2000). Human gelsolin prevents apoptosis by inhibiting apoptotic mitochondrial changes via closing VDAC. Oncogene *19*, 4807–4814.

Li, J., Li, Q., Xie, C., Zhou, H., Wang, Y., Zhang, N., Shao, H., Chan, S. C., Peng, X., Lin, S. C., and Han, J. (2004). Beta-actin is required for mitochondria clustering and ROS generation in TNF-induced, caspase-independent cell death. J. Cell Sci. *117*, 4673–4680.

Madeo, F., Frohlich, E., and Frohlich, K. U. (1997). A yeast mutant showing diagnostic markers of early and late apoptosis. J. Cell Biol. *139*, 729–734.

Madeo, F., Frohlich, E., Ligr, M., Grey, M., Sigrist, S. J., Wolf, D. H., and Frohlich, K. U. (1999). Oxygen stress: a regulator of apoptosis in yeast. J. Cell Biol. *145*, 757–767.

Mayer, M., and Noble, M. (1994). N-acetyl-L-cysteine is a pluripotent protector against cell death and enhancer of trophic factor-mediated cell survival in vitro. Proc. Natl. Acad. Sci. USA *91*, 7496–7500.

Morini, M., Cai, T., Aluigi, M. G., Noonan, D. M., Masiello, L., De Flora, S., D'Agostini, F., Albini, A., and Fassina, G. (1999). The role of the thiol N-acetylcysteine in the prevention of tumor invasion and angiogenesis. Int. J. Biol. Markers *14*, 268–271.

Okamoto, K., and Shaw, J. M. (2005). Mitochondrial morphology and dynamics in yeast and multicellular eukaryotes. Annu. Rev. Genet. *39*, 503–536.

Olave, I. A., Reck-Peterson, S. L., and Crabtree, G. R. (2002). Nuclear actin and actin-related proteins in chromatin remodeling. Annu. Rev. Biochem. *71*, 755–781.

Percipalle, P., and Visa, N. (2006). Molecular functions of nuclear actin in transcription. J. Cell Biol. *172*, 967–971.

Posey, S. C., and Bierer, B. E. (1999). Actin stabilization by jasplakinolide enhances apoptosis induced by cytokine deprivation. J. Biol. Chem. *274*, 4259–4265.

Rao, J., and Li, N. (2004). Microfilament actin remodeling as a potential target for cancer drug development. Curr. Cancer Drug Targets *4*, 345–354.

Rao, J. Y., Jin, Y. S., Zheng, Q., Cheng, J., Tai, J., and Hemstreet, G. P., 3rd. (1999). Alterations of the actin polymerization status as an apoptotic morphological effector in HL-60 cells. J. Cell Biochem. *75*, 686–697.

Roederer, M., Raju, P. A., Staal, F. J., and Herzenberg, L. A. (1991). N-acetylcysteine inhibits latent HIV expression in chronically infected cells. AIDS Res. Hum. Retroviruses *7*, 563–567.

Shartava, A., Korn, W., Shah, A. K., and Goodman, S. R. (1997). Irreversibly sickled cell beta-actin: defective filament formation. Am. J. Hematol. *55*, 97–103.

Shartava, A., Monteiro, C. A., Bencsath, F. A., Schneider, K., Chait, B. T., Gussio, R., Casoria-Scott, L. A., Shah, A. K., Heuerman, C. A., and Goodman, S. R. (1995). A posttranslational modification of beta-actin contributes to the slow dissociation of the spectrin-protein 4.1-actin complex of irreversibly sickled cells. J. Cell Biol. *128*, 805–818.

Sinclair, D., Mills, K., and Guarente, L. (1998). Aging in *Saccharomyces cerevisiae*. Annu. Rev. Microbiol. *52*, 533–560.

Susin, S. A. *et al.* (1999). Molecular characterization of mitochondrial apoptosis-inducing factor. Nature *397*, 441–446.

Wemmie, J. A., Steggerda, S. M., and Moye-Rowley, W. S. (1997). The *Saccharomyces cerevisiae* AP-1 protein discriminates between oxidative stress elicited by the oxidants H_2O_2 and diamide. J. Biol. Chem. *272*, 7908–7914.

Xu, X., Forbes, J. G., and Colombini, M. (2001). Actin modulates the gating of *Neurospora crassa* VDAC. J. Membr. Biol. *180*, 73–81.

Zyracka, E., Zadrag, R., Koziol, S., Krzepilko, A., Bartosz, G., and Bilinski, T. (2005). Ascorbate abolishes auxotrophy caused by the lack of superoxide dismutase in *Saccharomyces cerevisiae*. Yeast can be a biosensor for antioxidants. J. Biotechnol. *115*, 271–278.